Effect of Ginsenoside Rg1 on Renal Function and Its Signaling Pathway in an *in Vivo* and *in Vitro* Model of Sepsis

Jun Guo (qwek155@163.com)
Huazhong University of Science and Technology
Zhenhui Yuan
Huazhong University of Science and Technology
Rong Wang
Huazhong University of Science and Technology

Research Article

Keywords: Ginsenoside Rg1, Sepsis, Renal injury, Lipid peroxidation

Posted Date: March 11th, 2022

DOI: https://doi.org/10.21203/rs.3.rs-1421509/v1

Additional Declarations: No competing interests reported.

Abstract

Objective: To dissect the mechanism of the traditional Chinese medicine Ginsenoside Rg1 against sepsis-associated acute kidney injury (SAKI), we chose to investigate its contribution to the inhibition of lipid peroxidation and ferroptosis.

Methods: A SAKI animal model was used and urinary and serum samples were collected**.** Production of cytokines and biomarkers such as NGAL, KIM-1, IL-18 and IL-6 were examined by Enzyme-linked immunosorbent assay (ELISA). Proteins such as Gpx4, Ara70, and P53 levels were detected by western blot analysis. Intracellular reactive oxygen species (ROS) levels were also detected with specific dyes.

Results: We have established a cecal ligation and perforation (CLP) model to simulate SAKI in rats and showed that Rg1 treatment of this model could greatly mitigate the biomarkers of SAKI and progression of symptoms in vivo. In addition, we have shown that Rg1 treatment could reduce ROS level and ferroptosis to mitigate cell death in SAKI-derived cells and efficiently function as a protective agent against oxidation and ferroptosis. Finally, we demonstrated that Rg1 has the potential to be a potent cell death inhibitor as effective as Fer-1.

Conclusion: Altogether, we have identified a promising cell death inhibitor in SAKI that could exhibit potent activity as effective as Fer-1.

Introduction

Sepsis is one of the most important causes of acute kidney injury (AKI) in the intensive care units (ICU). Sepsis-associated AKI (SAKI) accounts for 15 ~ 20% of renal replacement therapy (RRT) in ICU and has been linked with an increased risk of chronic kidney disease (CKD), end-stage renal failure (ESRD) and very high mortality (1, 2). When RRT is used, the mortality rate can increase up to 80% or more (3).

Although septic shock is a leading cause of AKI, the underlying mechanisms of action are not fully understood. Up to date, the development of AKI has been attributed to not only inflammation responses, but also to ischemic/hypoxic and nephrotoxic changes to exotic insults such as cytokine activation or microcirculatory failure (4). Specifically, the pathophysiology of AKI in sepsis includes intrarenal hemodynamic changes, endothelial dysfunction, infiltration of inflammatory cells in the renal parenchyma, and obstruction of tubules with necrotic cells and debris (5, 6).

SAKI has shown distinct features in terms of pathophysiology (6), and this has led to the identification of a wide arrange of unique patterns of plasma and urinary biomarkers in septic AKI (2). For example, the secretion of IL-18 is higher in SAKI than in non-SAKI (7). In addition, both urinary netrin-1 and human kidney injury molecule type 1 (KIM-1) have been proven to be clinically useful as early biomarkers in the diagnosis of SAKI (8). Furthermore, plasma and urine concentrations of neutrophil gelatinase associated lipocalin (NGAL) and Cystatin C could also be treated as early diagnosis biomarkers of SAKI in critically ill

patients (9, 10). Besides, myo-inositol oxygenase (MIOX) as a proximal tubular enzyme was reported to exacerbate the pathogenesis progress of SAKI when MIOX overexpressing (11).

Lipid peroxidation plays an essential role in the development of SAKI (12). Lipid peroxidation can induce an imbalance in the prooxidant/antioxidant mechanism that promotes oxidative or nitrosative stress and finally triggers cytotoxicity (13). During oxidative stress, radical species such as lipid alkoxyl radical (LO·) and lipid peroxyl radical (LOO·) would promote lipid peroxidation and subsequently induce the synthesis of lipid peroxidation by-products (14). These by-products mediate DNA and/or protein alterations that cause kidney injury (15).

Accumulating lines of evidence demonstrated that application of traditional Chinese medicine (TCM) could improve AKI, and the mechanisms of action for some TCMs have been well illustrated (16). Among these, Ginsenoside Rd, isolated from the roots of *Panax ginseng*, was shown to protect cells in various types of diseases, especially ischemia diseases (17). Other Ginsenosides, such as Rg1, proved to be effective in the treatment of AKI and reduced aldosterone-induced oxidative stress and abnormal autophagy (18). However, the underlying genetic, cellular, and biochemical mode of action of Rg1 and related animal models are still lack of information.

In this study, we speculate that during SAKI, Rg1 could reduce the iron death of renal tubular epithelial cells by inhibiting lipid peroxidation. Specifically, we clarified the regulation of Rg1 on inflammation, oxidative stress, iron metabolism, and its role in the pathogenesis of SAKI, and established a SAKI animal model and compared the treatment of iron death inhibitors before and after cell damage. Overall, we have shown that Rg1 could be used as a potential drug against SAKI.

Materials And Methods

Chemicals and reagents

All chemicals and reagents used were purchased in analytical quality. The purity of the reference substances was >95%. Ginsenoside Rg1 (purity>95%) was purchased from Didakexiang Biological Co., Ltd (Guizhou, China) and dissolved in phosphate buffered saline (PBS) as a stock solution until further use. Fer-1 was purchased from DC Chemicals and used according to the manufacturer’s suggestion.

Ethics Statement

The following procedures were strictly faithful to 3R principles, and animal care and housing procedures were followed according to the Chinese regulatory requirements. The protocol used in this study was approved by the Ethics Committee of Union Jiangbei Hospital, Huazhong University of Science and Technology (HUST-LA0008). All tested animals received humane care in compliance with the Guide for the Care and Use of Laboratory Animals published by the National Institutes of Health.

Establishment of SAKI model

Healthy SD male rats (250-300 g) were chosen to establish the SAKI animal model. After the SD rats were kept in the laboratory for one week, cecal ligation and perforation were performed to establish a sepsis rat experimental model. All rats were divided into four groups (6 in each group): control group, model group, blank treatment group, Ginsenoside Rg1 treatment group. The Rg1 group was given by intraperitoneal injection of 125 mg/kg/d 24 h before cecal ligation. The blank treatment group was treated with cecal ligation. The same dose of normal saline as that of the Rg1 group was injected intraperitoneally one day before, and the model group was ligated and perforated in the cecum to establish a septic kidney injury rat model. After 1, 3, and 7 days after operation, after anesthesia, venous blood was collected by eyeball removal, rat urine and rat kidney tissue were collected for pathological examination.

Cell culture

Cells from the rat renal tubular epithelial cell and HK-2 cell line were cultured with BEGM Bronchial Epithelial Cell Growth Medium BulletKit (Lonza) or DEME/F12 medium containing 10% fetal bovine serum without antibiotics in a humidified incubator at 37°C with 5% CO_2. Stimulation with LPS (1 μg/mL) to HK-2 cells was performed for 24 h prior further examination.

Biochemical assays

Urinary samples were collected and the concentration of NGAL, KIM-1, and MIOX were measured using the enzyme linked immunosorbent assay (ELISA), according to the manufacturer's instructions. Serum was isolated after centrifugation at 3000 x g for 15 min. Measurement of IL-18 (ab213909, Abcam), IL-6 (ab234570, Abcam), and TNF-α (ab236712, Abcam) was performed by ELISA kits using pairs of specific mAbs and recombinant cytokine standards obtained from Invitrogen Life Technologies.

Histochemical staining

The kidney tissues of normal and Rg1 treated groups were collected separately and were stained with PAS (Periodic Acid-Schiff).

ROS analysis

Fluorescence-activated cell sorter (FACS) cytometry analysis was performed using the H_2O_2-activated green fluorescent dye, dihydro-dichloro-fluorescein diacetate (H_2DCFDA, Molecular Probes). This dye is readily taken up by cells, cleaved by cellular esterases to produce the noncell permeant H_2DCF, which can be activated by ROS giving green fluorescent DCF as an indication of intracellular levels of oxidative stress. Cell suspensions were adjusted to an OD600 of 0.5, pelleted by centrifugation, and resuspended in phosphate buffered saline (PBS) containing 20 mM H_2DCFDA. The suspension was incubated for 4 h, diluted 1:100 in PBS, and the fluorescence levels of 50,000 cells were recorded using a FACScalibur cytometer (BD Biosciences). Summit software (Dako Colorado) was used for data analysis.

Evaluation of iron level

To evaluate the ferroptosis level in different groups, iron concentrations in cell lysates were assessed using an Iron Assay Kit (Sigma-Aldrich, Cat #: MAK025) according to the manufacturer's instructions.

Cell viability assay

Cell viability assay was done according to the the instructions of CCK-8 kit (APExBIO). Briefly, 20 μL of the CCK-8 reagent was added to each well (containing 200 μL of medium) of a 96-well microplate, and the microplate was further incubated at 37℃ for 4 h. Finally, the OD (450 nm) were measured in different groups (n = 3). The cell viability in the control group (without any treatment) was regarded as "100%", and the relative cell viability of the other groups was calculated, respectively.

Western Blot Analysis

Concentrations of proteins were detected via a BCA protein assay kit (Sigma-Aldrich, Shanghai, China). Equal amounts of protein (20 μg) were loaded in each well and separated by 10% SDS-PAGE and blocked with 5% skimmed milk (BD) dissolved in TBST for 1 h, and then incubated with primary antibodies (anti-Gpx4, ARA70, P53, ERK1/2, Nrf2, p-Akt, GAPDH, 1:1000; Abcam, USA) at 4°C for 12 h. The membranes were washed three times for 7 min and incubated with the appropriate second antibody conjugate (Abcam, USA) or horseradish peroxidase-conjugated protein antibody (Sigma-Aldrich, Shanghai, China) for 1 h at room temperature. Then, the membranes were washed three times and stained with DAB Horseradish Peroxidase (Beyotime, Shanghai, China). The proteins were detected by using gel visualization (Tanon, Shanghai, China). Protein levels were normalized to GAPDH and quantified via densitometry.

LDH assay

Lactate dehydrogenase (LDH) was assessed with Lactate Dehydrogenase Activity Assay Kit (Sigma-Aldrich) according to the manufacturer's instructions.

Statistical analysis

Graphpad Prism software version 7 was used for all statistical analyses. The tests are indicated in the figure legends. Measured data are expressed as mean ± standard deviation and analyzed using the Student's *t*-test and variations considered significant at $p < 0.05$.

Results

Protective effect of Ginsenoside Rg1 on renal tissue in rats with sepsis

Considering the lack of animal models for the assessment of TCMs such as Ginsenoside Rg1 on SAKI, we have established an experimental model of SAKI in rats by using the cecal ligation and perforation (CLP) method. We aimed to use this SAKI model to observe the effects of Rg1 on the pathological changes of kidney tissues, serum creatinine, urea nitrogen levels, and urine KIM-1 and NGAL changes.

As can be seen from Fig. 1A, we have successfully shown that in urinary samples after 24 h CLP treatment, the CLP model group demonstrated a typical increase in the biomarkers such as NGAL, KIM-1, and MIOX. After treating with Rg1 and saline control, the increase of these biomarkers significantly decreased. In addition, we have examined the increase of several biomarkers such as IL-18, IL-6, and TNF-α and showed that CLP treatment led to substantial increase in these biomarkers and Rg1 treatment could result in the decrease of these biomarkers, strongly suggesting that Rg1 could be used as an efficient therapy against SAKI in our CLP model (Fig. 1B). To this aim, we performed pathological detection and found that Rg1 could indeed improve the kidney tissues from CLP injury (Fig. 1C) by using PAS staining.

Altogether, we have established one CLP model to simulate SAKI in rats and showed that Rg1 treatment of this model could greatly mitigate the biomarkers of SAKI and progression of symptoms in vivo.

Potential role of Ginsenoside Rg1 on lipid peroxidation and ferroptosis in renal tubular epithelial cells after sepsis

To understand the mechanisms of action of Rg1 against SAKI, we isolated the renal tubular epithelial cells to investigate oxidative stress related traits since it was reported that Rg1 could reduce aldosterone-induced oxidative stress (18). Firstly, we detected the reactive oxygen species (ROS) levels in CLP group compared to that of non-treatment control, we could clearly observe that more than 50% increase in ROS levels after CLP. After treated with Rg1, ROS levels significantly decreased compared to CLP group and saline control group (Fig. 2A). Since intracellular iron was involved in the formation of ROS and cell death called ferroptosis (19), we examined the iron levels in different treatment groups. As shown in Fig. 2B, the CLP group showed considerable elevation in intracellular iron levels compared to non-treatment controls. Interestingly, the application of Rg1 led to a more than 40% decrease in the intracellular iron levels (Fig. 2A), indicating that Rg1 could inhibit the iron-associated ferroptosis during SAKI.

We further investigated the biochemical mechanisms underlying Rg1-mediated inhibition of ferroptosis in SAKI. Firstly, we detected the expression of Gpx4 by using western blot analysis (Fig. 2B). We found that CLP treatment could lead to decreased expression of Gpx4 during SAKI while Rg1 treatment significantly reversed this reduction and restored the expression of Gpx4 to a regular level, explaining the reason of ferroptosis inhibition by Rg1. In addition, we assessed the expression of two cell death-related mediators, Ara70 and P53. As shown in Fig. 2B, we demonstrated that the CLP model showed increased expression of both mediators and Rg1 treatment of CLP cells resulted in the sharp attenuation of Ara70 and P53, as determined by western blot analysis.

In conclusion, we have shown that Rg1 treatment could reduce ROS and ferroptosis to mitigate cell death in SAKI-derived cells.

Effect of Ginsenoside Rg1 on lipid peroxidation and ferroptosis in HK-2 cells after LPS stimulation

To further prove the efficacy of Rg1 on lipid peroxidation and ferroptosis at the cellular level, we simulated the SAKI by using LPS (1 μg/ml) to stimulate HK-2 cells, a proximal tubular cell line derived

from the normal kidney. As can be seen from Fig. 3A, we can observe that CLP could clearly reduce the cell viability. However, after applying of Rg1 for 30 min and then stimulating HK-2 cells with LPS for 24 h, we found that Rg1 could efficiently rescue the LPS-induced cell death in a dose-dependent manner ranging from 10 to 100 μM.

Furthermore, we have determined the intracellular level of lactate dehydrogenase (LDH) to evaluate the cell damage. As shown in Fig. 3B, after LPS stimulation of HK-2 cell, CLP group showed the highest level of LDH activity compared to non-CLP control. While adding Rg1 to pretreat HK-2 cells, we found that LDH activity decreased more than 50% and showed a dose-dependent manner in LDH reduction. Finally, we demonstrated that Rg1 could attenuate the production of ROS and intracellular iron levels in LPS-stimulated HK-2 cells in a dose-dependent manner (Fig. 3C).

Taken together, we have proved that Rg1 could efficiently function as a protective agent against oxidation and ferroptosis.

Ginsenoside Rg1 inhibits expressions of ROS and GPX4, ARA70, and P53 comparable to existing ferroptosis inhibitor, Fer-1

As we have already established that Rg1 could effectively protect cells from damages from cell death induced by ferroptosis, we wonder whether the existing ferroptosis inhibitor could function together to protect therapy against SAKI-lined cell death. To do so, we used one of these inhibitors, Ferrostatin-1 (Fer-1) (20), to explore the possibility of combinatory application with Rg1.

As shown in Fig. 4A, we demonstrated that Fer-1 treatment of LPS-stimulated HK-2 cells revealed a relative reduction in ROS generation and intracellular iron levels. And this reduction was comparable to that of Rg1 treatment, with Rg1 as a better inhibitor during these processes. The combination of both Fer-1 and Rg1 did not have further effect on the reduction of ROS and iron levels in HK-2 cells.

Further biochemical analysis showed that Fer-1 could lead to the downregulation of Gpx4 in HK-2 cells and upregulation of cell death mediators Ara70 and P53 at translational levels (Fig. 4B). The effect of both these traits by Fer-1 was comparable to that of Rg1 treatment, demonstrating that Rg1 could be considered as a potent inhibitor drug during SAKI.

The inhibition of ROS-associated key regulators including ERK1/2, Nrf2, and p-Akt were investigated via WB analysis (Fig. 4C), we found that Fer-1 could lead to the downregulation of these proteins and the effect by Fer-1 was comparable to that of Rg1 treatment, demonstrating that Rg1 could be considered as a potent inhibitor drug during inflammation.

All in all, we have demonstrated that Rg1 has the potential to be a potent cell death inhibitor as effective as Fer-1.

Discussion

Sepsis is a serious medical disease characterized by a systemic inflammatory-response syndrome that could cause severe consequences, including multiple organ failure (2). Acute kidney injury (AKI) is a frequent complication of sepsis in intensive care unit (ICU) patients, especially in the elderly (21). Sepsis-associated AKI (SAKI) accounts for 15 ~ 20% of renal replacement therapy (RRT) in ICU and has been linked with an increased risk of chronic kidney disease (CKD), end-stage renal failure (ESRD) and a considerably high mortality (1, 2). When renal replacement therapy (RRT) is used, the mortality rate can increase up to 80% or more (3). Therefore, it is essential to search for efficient treatment against this medical threat.

In our study, we established a SAKI rat model that could demonstrate the typical pathophysiological traits characteristic of SAKI in humans. We have shown that in our SD rat model, a wide range of urinary and serum biomarkers such as NGAL, KIM-1, MIOX, IL-18, IL-6 and TNF-α were all revealed to be consistent with previously described trends (2, 22). Furthermore, we have evaluated the mechanism of one promising traditional Chinese medicine (TCM), Ginsenoside Rg1, against our SAKI rat model and found that Rg1 could function not only on inflammation, but also on the response of oxidative stress and iron metabolism in both animal model, renal tubular epithelial cell line, and LPS-stimulated HK-2 cell line in a dose-dependent manner. In addition, we have compared the treatment efficacy of iron death inhibitors such as Fer-1 with Rg1 and uncovered that Rg1 exhibited a relative superior performance to Fer-1, strongly suggesting that Rg1 could be used as a promising ferroptosis inhibitor and a potential drug against SAKI in mammalians.

It was previously reported that oxidative stress represents a hallmark in human sepsis and may be a link between microvascular failure and multiple-organ dysfunction (23, 24). In our study, we have identified one of the major proteins named Gpx4 (glutathione peroxidase 4), the expression of which has been significantly decreased in the SAKI model and inversely correlated with ROS generation and intracellular iron level, suggesting that downregulation of Gpx4 was indeed linked with iron-mediated ferroptosis in SAKI model (Fig. 2) (25, 26). In addition, the expression of Ara70 and P53, two important cell death mediators, were found to be highly expressed in SAKI model and positively correlated with cellular ROS and iron levels, implying that both mediators could be potential targets in treating against SAKI. Furthermore, we have shown that the expression of ERK1/2, Nfr2 and p-Akt, transcriptional regulators involved in oxidative stress, were all significantly affected by Rg1 (Fig. 4C) and this effect was enhanced by accompanying application of Fer-1. All these evidence suggested that Rg1 could potentially diminish the oxidative stress involved in SAKI.

Ginsenoside is a triterpenoid saponin predominantly extracted from *P. ginseng*, a traditional herbal medicine that is widely used in the world (27). As one of the most effective monomers, Ginsenoside Rg1, has been shown its medicinal value in the treatment of liver diseases (28), diabetes (27), neuronal diseases (29), and lung injury (30). The mechanistic mode of action of Rg1 was attributed to its anti-inflammatory and anti-apoptosis effects (31). This has been proved to be true in our SAKI model since Rg1 could mitigate the production of several immunological markers and cell death mediators such as Ara70 and P53 as well as the ROS and iron-mediated ferroptosis. Therefore, we have extended the

function of Rg1 in kidney diseases and primarily uncovered the mode of action of this important agent. In the future, we aim to further investigate the underlying biochemical analysis to determine further pathways involved in this protection. It was interesting to note that increasing the concentration of Rg1 exhibits a better protection effect on cell viability and cell damage. We speculate that this could further prove the protective role of Rg1 in anti-apoptosis. In addition to Rg1, we have also found that several other types of TCMs could be used as an efficient agent in treating SAKI, such as baicalin, resveratrol, and Ginsenoside Rd (18), indicating the great potential of TCMs in SAKI therapy.

Another interesting finding from our study was the efficacy of Rg1, which could be comparable to that of Fer-1, a well-known ferroptosis inhibitor (20). We have shown in our study that Rg1 demonstrated better efficacy in defense against ferroptosis (Fig. 4A). We have proved this by biochemical investigations, further strengthening the role of Rg1 in defense against ROS and ferroptosis in our SAKI model. In the future, we would like to reproduce this in multiple cell lines and extend the use of Rg1 in different diseases. Besides, we have noticed that the combination of Fer-1 and Rg1 showed no significant increase in the defense against ROS and ferroptosis in HK-2 cells. This was unexpected since we aimed to determine the synergy between both agents and further extend the use of this combination. The probable reason for this is the mode of action of Fer-1 and Rg1 coincide with each other and no synergistic effect could be observed when both agents were applied in the same target(s). However, this would not affect the potential use of Rg1 as a promising drug for the treatment of SAKI in mammalians.

Conclusion

Sepsis-associated AKI (SAKI) accounts for 15 ~ 20% of renal replacement therapy (RRT) in ICU and has been linked to high mortality. Therefore, it is essential to search for efficient treatment against this disease. In our study, we established a SAKI rat model that precisely demonstrated the typical pathophysiological traits characteristic of SAKI. Furthermore, we dissected the mechanism of traditional Chinese medicine Ginsenoside Rg1against SAKI model and found that Rg1 could function on inflammation, oxidative stress, and iron metabolism. This protection was observed in both the animal model and renal tubular epithelial cells and LPS-stimulated HK-2 cells, implying Rg1 was functional in different cellular niches. In addition, we have compared the treatment of iron death inhibitors such as Fer-1 before and after cell damage with Rg1 and Rg1 showed a better performance as efficient as Fer-1. Overall, we have shown that Rg1 could be used as a promising cell death inhibitor and potential drug against SAKI.

Declarations

Acknowledgement

None.

Contributions

Writing - original draft: Jun Guo.

Writing - review & editing: Jun Guo;

Designed and performed the experiments: Jun Guo;

Statistical analysis: Zhenhui Yuan, Rong Wang;

All authors read and approved the final manuscript.

Competing interest

The authors have no competing interests to declare.

References

1. Uchino S, Kellum JA, Bellomo R, Doig GS, Morimatsu H, Morgera S, Schetz M, Tan I, Bouman C, Macedo E, Gibney N, Tolwani A, Ronco C, Beginning, Ending Supportive Therapy for the Kidney I. 2005. Acute renal failure in critically ill patients: a multinational, multicenter study. *JAMA* 294:813-8.
2. Zarjou A, Agarwal A. 2011. Sepsis and acute kidney injury. *J Am Soc Nephrol* 22:999-1006.
3. Schrier RW, Wang W, Poole B, Mitra A. 2004. Acute renal failure: definitions, diagnosis, pathogenesis, and therapy. *J Clin Invest* 114:5-14.
4. Doi K. 2016. Role of kidney injury in sepsis. *J Intensive Care* 4:17.
5. Shum HP, Yan WW, Chan TM. 2016. Recent knowledge on the pathophysiology of septic acute kidney injury: A narrative review. *J Crit Care* 31:82-9.
6. Wan L, Bagshaw SM, Langenberg C, Saotome T, May C, Bellomo R. 2008. Pathophysiology of septic acute kidney injury: what do we really know? *Crit Care Med* 36:S198-203.
7. Bagshaw SM, Langenberg C, Haase M, Wan L, May CN, Bellomo R. 2007. Urinary biomarkers in septic acute kidney injury. *Intensive Care Med* 33:1285-1296.
8. Tu Y, Wang H, Sun R, Ni Y, Ma L, Xv F, Hu X, Jiang L, Wu A, Chen X, Chen M, Liu J, Han F. 2014. Urinary netrin-1 and KIM-1 as early biomarkers for septic acute kidney injury. *Ren Fail* 36:1559-63.
9. Bagshaw SM, Bennett M, Haase M, Haase-Fielitz A, Egi M, Morimatsu H, D'Amico G, Goldsmith D, Devarajan P, Bellomo R. 2010. Plasma and urine neutrophil gelatinase-associated lipocalin in septic versus non-septic acute kidney injury in critical illness. *Intensive Care Med* 36:452-61.
10. Aydogdu M, Gursel G, Sancak B, Yeni S, Sari G, Tasyurek S, Turk M, Yuksel S, Senes M, Ozis TN. 2013. The use of plasma and urine neutrophil gelatinase associated lipocalin (NGAL) and Cystatin C in early diagnosis of septic acute kidney injury in critically ill patients. *Dis Markers* 34:237-46.
11. Deng F, Sharma I, Dai Y, Yang M, Kanwar YS. 2019. Myo-inositol oxygenase expression profile modulates pathogenic ferroptosis in the renal proximal tubule. *J Clin Invest* 129:5033-5049.

12. Nara A, Yajima D, Nagasawa S, Abe H, Hoshioka Y, Iwase H. 2016. Evaluations of lipid peroxidation and inflammation in short-term glycerol-induced acute kidney injury in rats. *Clin Exp Pharmacol Physiol* 43:1080-1086.
13. Mata-Miranda MM, Bernal-Barquero CE, Martinez-Cuazitl A, Guerrero-Robles CI, Sanchez-Monroy V, Rojas-Lopez M, Vazquez-Zapien GJ. 2019. Nephroprotective Effect of Embryonic Stem Cells Reducing Lipid Peroxidation in Kidney Injury Induced by Cisplatin. *Oxid Med Cell Longev* 2019:5420624.
14. Panizo N, Rubio-Navarro A, Amaro-Villalobos JM, Egido J, Moreno JA. 2015. Molecular Mechanisms and Novel Therapeutic Approaches to Rhabdomyolysis-Induced Acute Kidney Injury. *Kidney Blood Press Res* 40:520-32.
15. Reeder BJ, Wilson MT. 2005. Hemoglobin and myoglobin associated oxidative stress: from molecular mechanisms to disease States. *Curr Med Chem* 12:2741-51.
16. Li HD, Meng XM, Huang C, Zhang L, Lv XW, Li J. 2019. Application of Herbal Traditional Chinese Medicine in the Treatment of Acute Kidney Injury. *Front Pharmacol* 10:376.
17. Ye R, Yang Q, Kong X, Han J, Zhang X, Zhang Y, Li P, Liu J, Shi M, Xiong L, Zhao G. 2011. Ginsenoside Rd attenuates early oxidative damage and sequential inflammatory response after transient focal ischemia in rats. *Neurochem Int* 58:391-8.
18. Zhu Y, Fu Y, Lin H. 2016. Baicalin Inhibits Renal Cell Apoptosis and Protects Against Acute Kidney Injury in Pediatric Sepsis. *Med Sci Monit* 22:5109-5115.
19. Park E, Chung SW. 2019. ROS-mediated autophagy increases intracellular iron levels and ferroptosis by ferritin and transferrin receptor regulation. *Cell Death Dis* 10:822.
20. Skouta R, Dixon SJ, Wang J, Dunn DE, Orman M, Shimada K, Rosenberg PA, Lo DC, Weinberg JM, Linkermann A, Stockwell BR. 2014. Ferrostatins inhibit oxidative lipid damage and cell death in diverse disease models. *J Am Chem Soc* 136:4551-6.
21. Lafrance JP, Miller DR. 2010. Acute kidney injury associates with increased long-term mortality. *J Am Soc Nephrol* 21:345-52.
22. Wang K, Xie S, Xiao K, Yan P, He W, Xie L. 2018. Biomarkers of Sepsis-Induced Acute Kidney Injury. *Biomed Res Int* 2018:6937947.
23. Gomez H, Ince C, De Backer D, Pickkers P, Payen D, Hotchkiss J, Kellum JA. 2014. A unified theory of sepsis-induced acute kidney injury: inflammation, microcirculatory dysfunction, bioenergetics, and the tubular cell adaptation to injury. *Shock* 41:3-11.
24. Eleftheriadis T, Pissas G, Filippidis G, Liakopoulos V, Stefanidis I. 2021. Reoxygenation induces reactive oxygen species production and ferroptosis in renal tubular epithelial cells by activating aryl hydrocarbon receptor. *Mol Med Rep* 23.
25. Friedmann Angeli JP, Schneider M, Proneth B, Tyurina YY, Tyurin VA, Hammond VJ, Herbach N, Aichler M, Walch A, Eggenhofer E, Basavarajappa D, Radmark O, Kobayashi S, Seibt T, Beck H, Neff F, Esposito I, Wanke R, Forster H, Yefremova O, Heinrichmeyer M, Bornkamm GW, Geissler EK, Thomas

SB, Stockwell BR, O'Donnell VB, Kagan VE, Schick JA, Conrad M. 2014. Inactivation of the ferroptosis regulator Gpx4 triggers acute renal failure in mice. *Nat Cell Biol* 16:1180-91.

26. Imai H, Matsuoka M, Kumagai T, Sakamoto T, Koumura T. 2017. Lipid Peroxidation-Dependent Cell Death Regulated by GPx4 and Ferroptosis. *Curr Top Microbiol Immunol* 403:143-170.
27. Li L, Yang N, Nin L, Zhao Z, Chen L, Yu J, Jiang Z, Zhong Z, Zeng D, Qi H, Xu X. 2015. Chinese herbal medicine formula tao hong si wu decoction protects against cerebral ischemia-reperfusion injury via PI3K/Akt and the Nrf2 signaling pathway. *J Nat Med* 69:76-85.
28. Ning C, Gao X, Wang C, Kong Y, Liu Z, Sun H, Sun P, Huo X, Ma X, Meng Q, Liu K. 2018. Ginsenoside Rg1 protects against acetaminophen-induced liver injury via activating Nrf2 signaling pathway in vivo and in vitro. *Regul Toxicol Pharmacol* 98:58-68.
29. Xu TZ, Shen XY, Sun LL, Chen YL, Zhang BQ, Huang DK, Li WZ. 2019. Ginsenoside Rg1 protects against H2O2induced neuronal damage due to inhibition of the NLRP1 inflammasome signalling pathway in hippocampal neurons in vitro. *Int J Mol Med* 43:717-726.
30. Ye Y, Shan Y, Bao C, Hu Y, Wang L. 2018. Ginsenoside Rg1 protects against hind-limb ischemia reperfusion induced lung injury via NF-kappaB/COX-2 signaling pathway. *Int Immunopharmacol* 60:96-103.
31. Xu Y, Yang C, Zhang S, Li J, Xiao Q, Huang W. 2018. Ginsenoside Rg1 Protects against Non-alcoholic Fatty Liver Disease by Ameliorating Lipid Peroxidation, Endoplasmic Reticulum Stress, and Inflammasome Activation. *Biol Pharm Bull* 41:1638-1644.

Figures

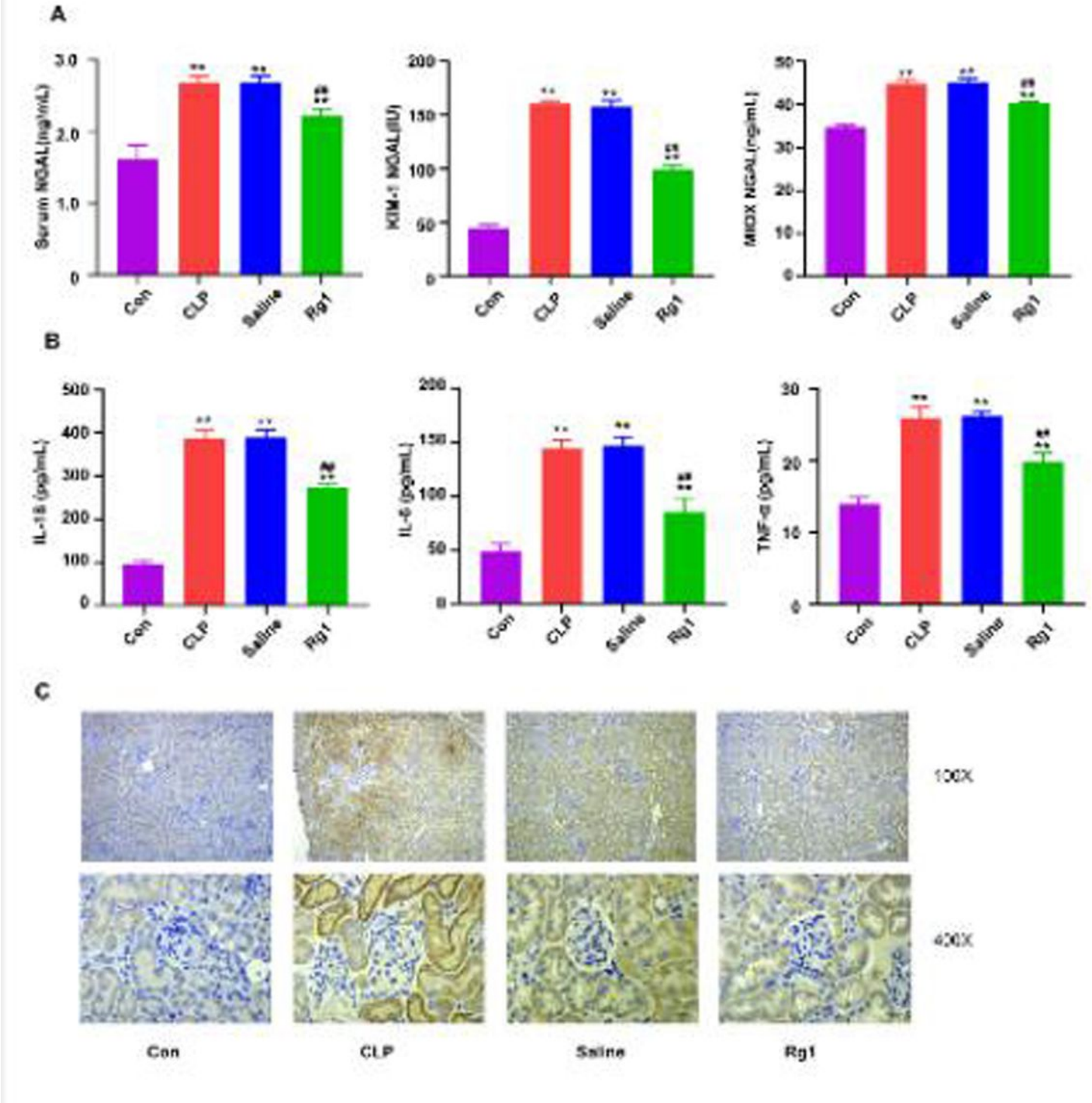

Figure 1

Protective effect of Ginsenoside Rg1 on renal tissue in rats with sepsis

A. Urinary NGAL, KIM-1 and MIOX levels in collected rat urine samples. Rg1 treatment and other control groups were performed as described in Materials and Methods section (See Materials and methods). Con, control group; CLP, model group; Saline, model group treated with saline; Rg1, model group treated with

Rg1. Results were expressed as mean ± SD (n = 6), and *P* value less than 0.05 was considered statistically significant. **, *P*<0.01 vs Con group; ## *P*<0.01 vs CLP group.

B. Serum IL-18, IL-6, and TNF-α levels in collected rat serum samples. Rg1 treatment and other control groups were performed as described in Materials and Methods section (See Materials and methods). Con, control group; CLP, model group; Saline, model group treated with saline; Rg1, model group treated with Rg1. Results were expressed as mean ± SD (n = 6), and *P* value less than 0.05 was considered statistically significant. **, *P*<0.01 vs Con group; ## *P*<0.01 vs CLP group.

C. Pathological detection of kidney tissues stained with PAS. Con, control group; CLP, model group; Saline, model group treated with saline; Rg1, model group treated with Rg1. Results were representative of three replicates of each group.

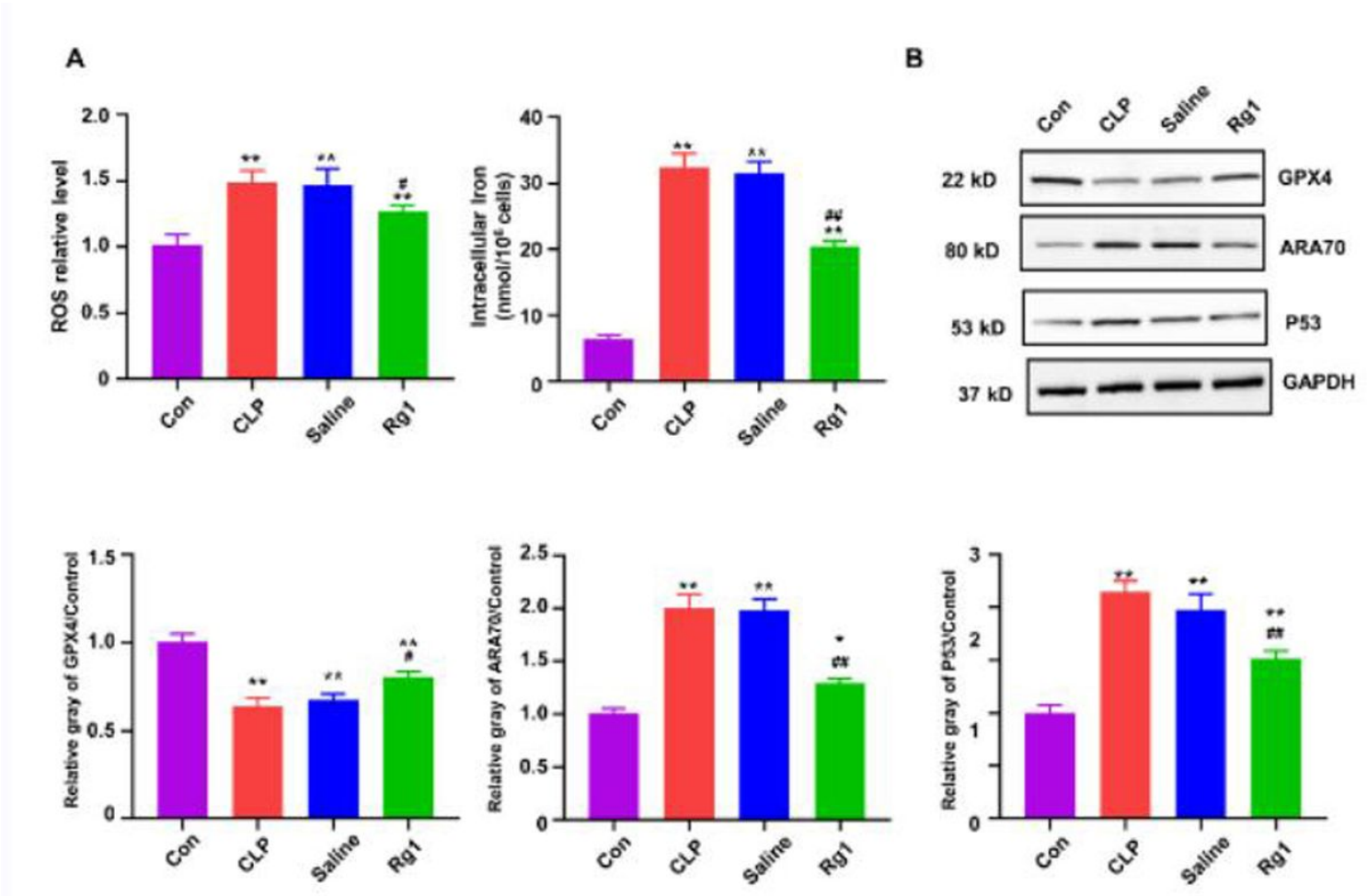

Figure 2

Potential role of Ginsenoside Rg1 on lipid peroxidation and ferroptosis in renal tubular epithelial cells after sepsis

A. Relative ROS and iron levels in renal tubular epithelial cells after sepsis. ROS was quantified as a relative level as compared to that of control group. Con, control group; CLP, model group; Saline, model

group treated with saline; Rg1, model group treated with Rg1. Results were expressed as mean ± SD (n = 3), and *P* value less than 0.05 was considered statistically significant. **, *P*<0.01 vs Con group; ## *P*<0.01 vs CLP group.

B. Cells were collected at 24 h post Rg1 treatment and evaluated by western blotting analysis for Gpx4, Ara70, and P53 proteins. GAPDH was used as a housekeeping control. Molecular weight of each protein was labelled alongside the corresponding band. The relative quantification of immunoblot was calculated downside of each blot. Con, control group; CLP, model group; Saline, model group treated with saline; Rg1, model group treated with Rg1. Quantitative results were expressed as mean ± SD (n = 3), and *P* value less than 0.05 was considered statistically significant. **, *P*<0.01 vs Con group; *, *P*<0.05 vs Con group; ## *P*<0.01 vs CLP group; # *P*<0.05 vs CLP group.

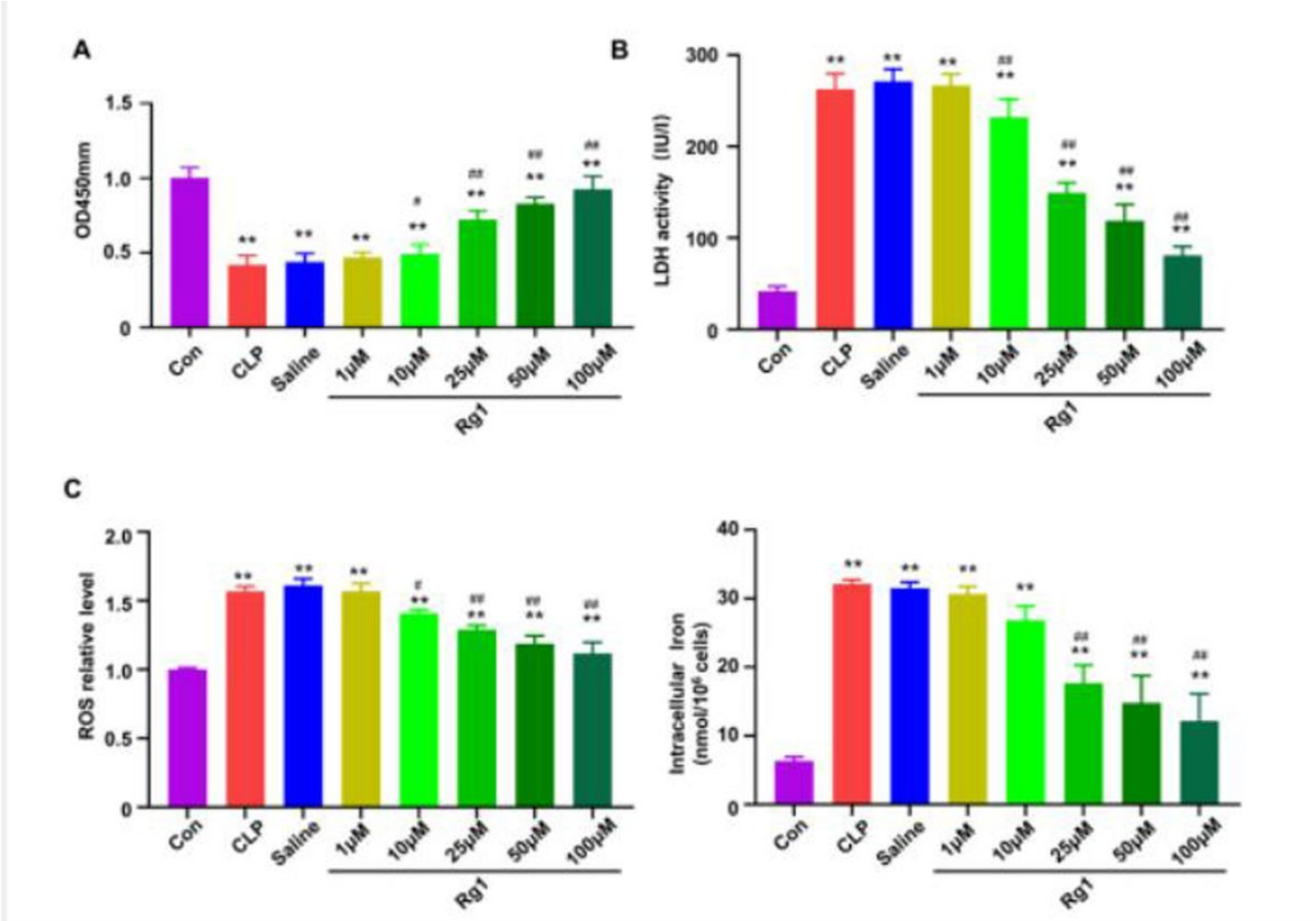

Figure 3

Effect of Ginsenoside Rg1 on lipid peroxidation and ferroptosis in HK-2 cells after LPS stimulation

A. Cell viability was evaluated using CCK-8 method. Results were expressed as mean ± SD (n = 3), and *P* value less than 0.05 was considered statistically significant. Con, control group; CLP, model group; Saline,

model group treated with saline; Rg1, model group treated with Rg1. **, *P*<0.01 vs Con group; ## *P*<0.01 vs CLP group; # *P*<0.05 vs CLP group.

B. LDH assay of Rg1 treatment. Cells were collected at 24 h post Rg1 treatment and evaluated by LDH analysis for cell damage. Results were expressed as mean ± SD (n = 3), and *P* value less than 0.05 was considered statistically significant. Con, control group; CLP, model group; Saline, model group treated with saline; Rg1, model group treated with Rg1. **, *P*<0.01 vs Con group; ## *P*<0.01 vs CLP group.

C. Relative ROS and iron levels in HK-2 cell after LPS (1 μg/ml) stimulation. ROS was quantified as a relative level as compared to that of control group. Con, control group; CLP, model group; Saline, model group treated with saline; Rg1, model group treated with Rg1. Results were expressed as mean ± SD (n = 3), and *P* value less than 0.05 was considered statistically significant. **, *P*<0.01 vs Con group; ## *P*<0.01 vs CLP group; # *P*<0.05 vs CLP group.

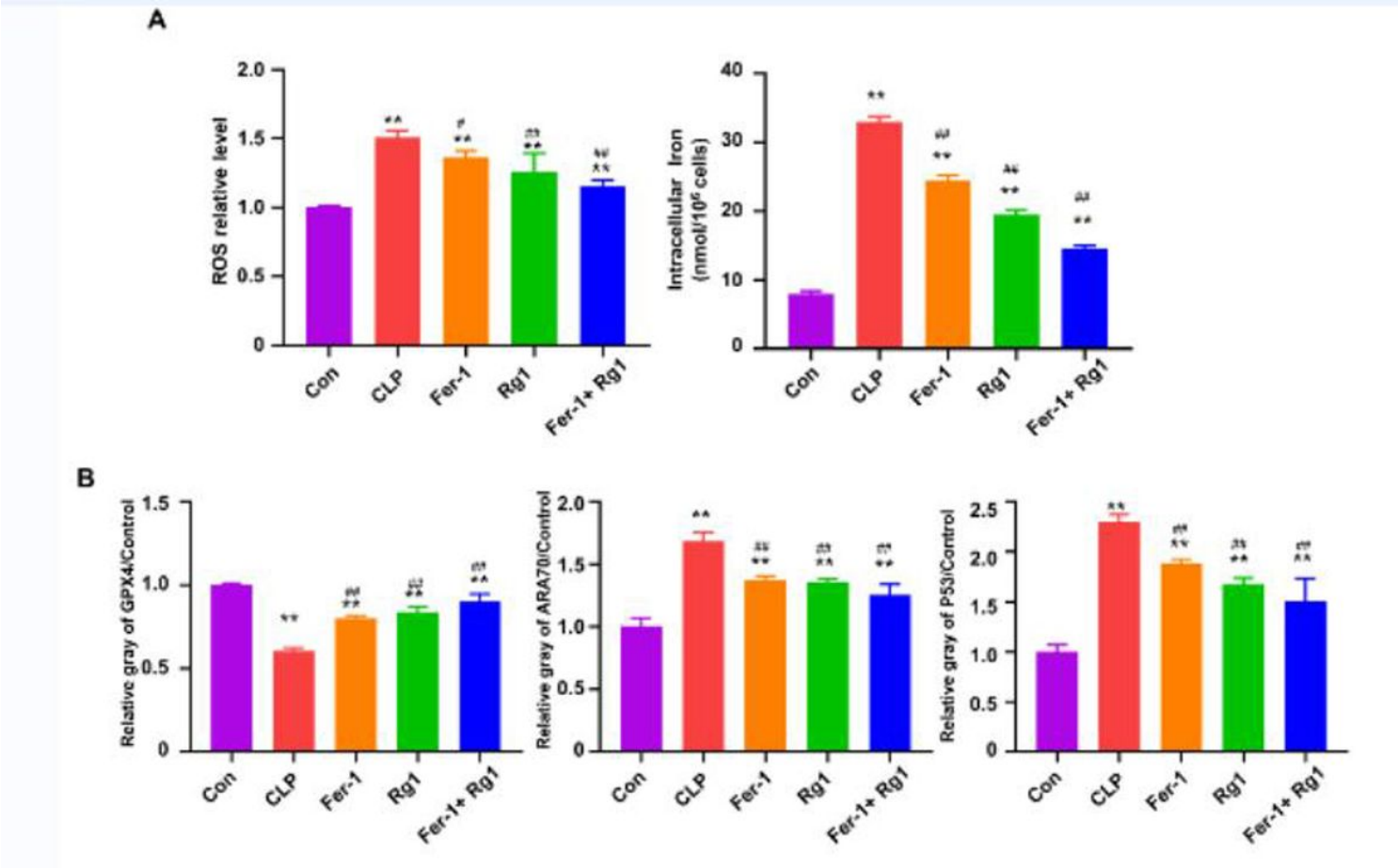

Figure 4

Ginsenoside Rg1 inhibits expressions of ROS and GPX4, ARA70, and P53 comparable to existing ferroptosis inhibitor, Fer-1

A. Relative ROS and iron levels in HK-2 cell after LPS (1 μg/ml) stimulation. ROS was quantified as a relative level as compared to that of control group. Con, control group; CLP, model group; Fer-1, model

group treated with Fer-1; Rg1, model group treated with Rg1; Fer-1+Rg1, combination treatment with Fer-1 and Rg1. Results were expressed as mean ± SD (n = 3), and *P* value less than 0.05 was considered statistically significant. **, *P*<0.01 vs Con group; ## *P*<0.01 vs CLP group; # *P*<0.05 vs CLP group.

B. Cells were collected at 24 h post inhibitor treatment and evaluated by western blotting analysis for Gpx4, Ara70 and P53 proteins. GAPDH was used as a housekeeping control. Molecular weight of each protein was labelled alongside the corresponding band. The relative quantification of immunoblots was calculated downside of each blot. Con, control group; CLP, model group; Fer-1, model group treated with Fer-1; Rg1, model group treated with Rg1; Fer-1+Rg1, combination treatment with Fer-1 and Rg1. Quantitative results were expressed as mean ± SD (n = 3), and *P* value less than 0.05 was considered statistically significant. **, *P*<0.01 vs Con group; *, *P*<0.05 vs Con group; ## *P*<0.01 vs CLP group.

C. Cells were collected at 24 h post inhibitor treatment and evaluated by western blotting analysis for ERK1/2, Nrf2 and p-Akt proteins. GAPDH was used as a housekeeping control. Molecular weight of each protein was labelled alongside the corresponding band. Con, control group; CLP, model group; Fer-1, model group treated with Fer-1; Rg1, model group treated with Rg1; Fer-1+Rg1, combination treatment with Fer-1 and Rg1.